Zero-energy modes and gate-tunable gap in graphene on hexagonal boron nitride

M. Kindermann, Bruno Uchoa, and D. L. Miller

Phys. Rev. B **86**, 115415 — Published 13 September 2012

DOI: 10.1103/PhysRevB.86.115415

Zero Energy Modes and Gate-Tunable Gap in Graphene on hexagonal Boron Nitride

M. Kindermann[1], Bruno Uchoa[2] and D. L. Miller[3]

[1] *School of Physics, Georgia Institute of Technology, Atlanta, Georgia 30332, USA*
[2] *Department of Physics and Astronomy, University of Oklahoma, Norman, OK 73069, USA and*
[3] *National Institute of Standards and Technology, Boulder, CO 80305 USA*

In this article, we derive an effective theory of graphene on a hexagonal Boron Nitride (h-BN) substrate. We show that the h-BN substrate generically opens a spectral gap in graphene despite the lattice mismatch. The origin of that gap is particularly intuitive in the regime of strong coupling between graphene and its substrate, when the low-energy physics is determined by the topology of a network of zero energy modes. For twisted graphene bilayers, where inversion symmetry is present, this network percolates through the system and the spectrum is gapless. The breaking of that symmetry by h-BN causes the zero energy modes to close into rings. The eigenstates of these rings hybridize into flat bands with gaps in between. The size of this band gap can be tuned by a gate voltage and it can reach the order of magnitude needed to confine electrons at room temperature.

PACS numbers: 73.20.-r,73.22.Pr,79.60.Jv

INTRODUCTION

Graphene is a two-dimensional semimetal with low-energy excitations that obey the massless Dirac equation [1–3]. As most applications in electronics require a bandgap, much effort has been exerted to find ways of inducing a gap in the electronic spectrum of graphene. One possible route is to use hexagonal boron nitride (h-BN) substrates [4, 5], which lack sublattice inversion symmetry. If inherited by the graphene layer, this broken symmetry leads to the opening of a gap in the spectrum, which is described by a mass in the Dirac model. First principles calculations for graphene supported by a perfectly lattice matched h-BN substrate predicted a bandgap on the order 50 meV [4]. Experiments, however, have not observed any clear indication of a gap [6, 7].

Subsequent theory [8, 9] identified the reason for this discrepancy: the lattice constants of h-BN and graphene differ by about 1.8% and for multi-layered h-BN substrates it is energetically unfavorable for graphene and its substrate to conform their lattice constants [8]. The result is Moiré patterns of varying local lattice alignment, as illustrated in Fig. 1, which have been observed in scanning tunneling microscopy [10]. Evidently, the h-BN substrate breaks sublattice symmetry differently in different regions of the Moiré pattern. Density functional theory (DFT) calculations have shown a tendency for the sublattice symmetry breaking to be compensated between different regions of the Moiré pattern such that the symmetry is almost restored after spatial average [8]. This has motivated the proposal of effective Dirac models of graphene on h-BN with a mass term that has vanishing integral, such that sublattice inversion symmetry is restored on (spatial) average. On the basis of those models, it was argued that a band gap in graphene on h-BN is absent [8, 9], consistently with the existing experimental data [6, 7].

In this article, we derive an effective theory for graphene on h-BN based on a bilayer model that has been successfully applied to twisted graphene bilayers [11–13]. Our theory is formulated for a single-layer of graphene and it accounts for the coupling to the substrate by a mass term and effective potentials that oscillate with the period of the Moiré pattern. We find that graphene supported by a hexagonal substrate generically develops a gap in the spectrum. In particular, the emergence of a spectral gap is *not* precluded by an average sublattice symmetry. A gap is avoided only by additional symmetries, such as in twisted graphene bilayers, where the Dirac points are topologically protected by a combination of space inversion and time reversal symmetry [14]. The magnitude of this gap under typical conditions is, however, smaller than the resolution of all previous experiments [6, 7] and has therefore not been observed, yet.

In the regime of strong coupling between graphene and its substrate a particularly intuitive picture of that gap formation emerges: the oscillatory mass in our effective theory then defines one-dimensional modes that are topologically protected and gapless for a large Moiré period. In the presence of space inversion symmetry, such as in twisted graphene bilayers, these modes form a network that percolates through the system, corresponding to a metallic state. When space inversion symmetry is bro-

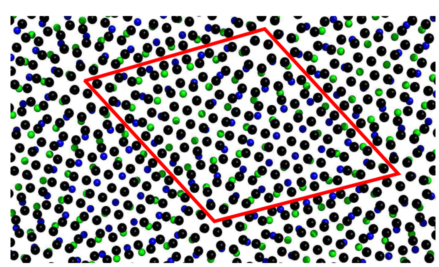

FIG. 1: Two layer system made of graphene (top layer) and h-BN (bottom layer) with a lattice mismatch (exaggerated in the figure). Red line: Moiré unit cell of the system.

ken, for instance by h-BN, this network breaks up into isolated rings of 1D-modes. The states in these rings hybridize exponentially weakly and form narrow bands with large gaps set by the level spacing in the rings.

Finally, we show that the spectral gap of graphene on h-BN can be controlled by the application of a perpendicular electric field. Using parameters fitted to experiments and DFT calculations, we find that the gap can be tuned to reach the order of magnitude needed to confine charge carriers at room temperature, a key requirement for electronics applications.

MODEL

We base our analysis of graphene with an h-BN substrate on a tight-binding model of two coupled honeycomb lattices with parameters fitted to experiment [15]. The two layers have a lattice mismatch of $\delta \approx 1.8\%$ (cf. Fig. 1) and we allow in addition a rotational misalignment by angle θ. In the two-layer basis of graphene and h-BN, the electronic Hamiltonian is

$$H = \begin{pmatrix} H_{\mathrm{g}} & H_{\mathrm{int}} \\ H_{\mathrm{int}}^{\dagger} & H_{\mathrm{BN}} \end{pmatrix}. \tag{1}$$

In the limit $\theta \ll 1$ and $\delta \ll 1$, where a long-wavelength description is appropriate, the isolated graphene layer can be described by a Dirac model Hamiltonian $H_{\mathrm{g}} = v\mathbf{p}\cdot\mathbf{\Sigma}$, and the h-BN layer is similarly described by $H_{\mathrm{BN}} = v_{\mathrm{BN}}\mathbf{p}\cdot\mathbf{\Sigma} + mv^2\sigma_z + V$ [5], where v and v_{BN} are the carrier velocities in graphene and h-BN, respectively and $\mathbf{p}$ is the momentum relative to the Dirac points. H_{g} and H_{BN} each act on 4 component spinors of the form $(\psi_{\mathrm{A},+}, \psi_{\mathrm{B},+}, \psi_{\mathrm{A},-}, \psi_{\mathrm{B},-})$, with A, B labeling the two different sublattices of the honeycomb lattice and $\pm$ denoting the two different band structure valleys. $\mathbf{\Sigma} = (\tau_z\sigma_x, \sigma_y)$ is a vector of Pauli matrices acting on the A/B sublattice basis (through the pseudospin $\boldsymbol{\sigma}$) and the valley spin ($\boldsymbol{\tau}$). The mass m and the interlayer bias V account for the different on-site potentials of the Boron (the A sublattice of h-BN) and the Nitrogen (B-)atoms. DFT calculations indicate $mv^2 \approx 2.3\,\mathrm{eV}$ and $V \approx 0.8\,\mathrm{eV}$ [5]. The bias V can be tuned by a perpendicular electric field.

Following Ref. [13], we take the interlayer coupling of Eq. (1) at long-wavelengths to be of the form [11, 13]

$$H_{\mathrm{int}} = \frac{\gamma}{3}\sum_n e^{i\tau_z \delta\boldsymbol{K}_n\cdot\boldsymbol{r}} \begin{pmatrix} 1 & \zeta\, e^{i\tau_z\phi_n} \\ \zeta\, e^{-i\tau_z\phi_n} & 1 \end{pmatrix}. \tag{2}$$

Here, H_{int} is written explicitly in the A, B sublattice basis, $\gamma \approx 0.3$ eV is the hopping energy to the substrate, ζ parametrizes a sublattice asymmetry due to structural differences between different regions of the Moiré pattern [13], and $\phi_n = 2\pi n/3$ is a phase that depends on the index $n = 0, 1, 2$, which labels the three corners of the graphene Brillouin zone corresponding to a given valley. Those points have wavevectors $\boldsymbol{K}_n = R(\phi_n + \pi/6)\hat{a}\, 4\pi/3\sqrt{3a}$, where $\hat{a}$ is a unit vector along an A-B bond, a the bond length, and $R(\varphi)$ is a rotation by angle φ. The wavevectors $\delta\boldsymbol{K}_n$ are the differences of $\boldsymbol{K}_n$ and their counterparts in the closest valley of the h-BN layer. They are shorter than $\boldsymbol{K}_n$ by a factor $\delta K_n/K_n = \sqrt{\delta^2 - 2(1+\delta)(\cos\theta - 1)}/(1+\delta)$ and rotated with respect to $\boldsymbol{K}_n$ by angle $\Phi = \arctan\left[\sin\theta/(1+\delta-\cos\theta)\right]$. We neglect commensuration effects, which are small for $\delta, \theta \ll 1$ [16].

EFFECTIVE SINGLE-LAYER THEORY

Integrating out the electrons in the h-BN layer, we arrive at an effective Hamiltonian $H_{\mathrm{g}}^{\mathrm{eff}}(\omega) = H_{\mathrm{g}} + \delta H_{\mathrm{g}}^{\mathrm{eff}}(\omega)$ for the graphene layer with (we set $\hbar = 1$)

$$\delta H_{\mathrm{g}}^{\mathrm{eff}}(\omega) = H_{\mathrm{int}}(\omega - H_{\mathrm{BN}})^{-1} H_{\mathrm{int}}^{\dagger}. \tag{3}$$

The mass term m dominates the Hamiltonian H_{BN} for all wavevectors where the employed Dirac model holds. At those momenta, $p \ll K_n$, we may set $v_{\mathrm{BN}} = 0$ to a good approximation, resulting in an effective Hamiltonian which is local in space [20],

$$\delta H_{\mathrm{g}}^{\mathrm{eff}} = \frac{1}{\omega - V + mv^2} H_{\mathrm{int}} \begin{pmatrix} \eta & 0 \\ 0 & 1 \end{pmatrix} H_{\mathrm{int}}^{\dagger}, \tag{4}$$

where η parametrizes the inversion symmetry breaking through the h-BN substrate,

$$\eta = (\omega - V + mv^2)/(\omega - V - mv^2). \tag{5}$$

The effective Hamiltonian (4) can be parametrized in terms of effective potentials that oscillate in space with the periodicity of the bilayer Moiré pattern,

$$\delta H_{\mathrm{g}}^{\mathrm{eff}} = V^{\mathrm{eff}}(\mathbf{r}) + \nu v e \mathbf{\Sigma}\cdot\boldsymbol{A}^{\mathrm{eff}}(\mathbf{r}) + m^{\mathrm{eff}}(\mathbf{r})v^2\sigma_z. \tag{6}$$

For perfect rotational alignment, $\theta = \Phi = 0$, the effective vector potential $\boldsymbol{A}^{\mathrm{eff}}$ may be gauged away. In the more general case $\Phi \neq 0$ the vector potential generates a pseudo-magnetic field and it satisfies the Coulomb gauge condition $\boldsymbol{\nabla}\cdot\boldsymbol{A}^{\mathrm{eff}} = 0$ at $\Phi = \pi/2$. The mass term $m^{\mathrm{eff}}(\mathbf{r})$ breaks the sublattice exchange symmetry locally and it opens a local gap in the spectrum wherever it exceeds $1/vL$, such that the wavefunctions are localized on the length scale L of the Moiré pattern.

A global gap in the spectrum is nevertheless precluded when the effective theory Eq. (4) is invariant under $P = \sigma_x\tau_x R(\pi)$ [21], that is sublattice exchange σ_x coupled with point reflection $R(\pi)$ and valley exchange τ_x, such that the underlying lattice model has inversion and time reversal symmetry, as for twisted graphene bilayers. In the following, we analyze the spectral gap of graphene on h-BN in the absence of that symmetry, which is explicitly broken by the inequivalence of the B and N sites.

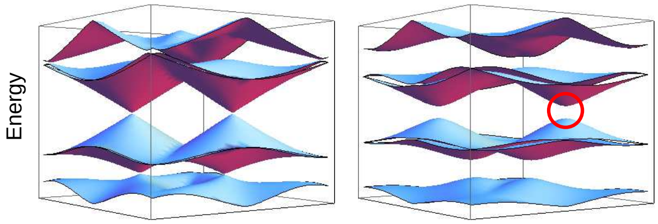

FIG. 2: Energy spectra in the Moiré Brillouin zone for strong coupling $\varepsilon = L\gamma^2/[(V - mv^2)v] \gg 1$. (Left) $\eta = 1$, as in twisted graphene bilayers (corresponding to the triangular network of zero energy modes shown in Fig. 3 a), with a metallic spectrum. (Right) $\zeta = 1$ and $\eta = -0.5$ (corresponding to isolated rings of low-energy modes, as shown in Fig. 3 b-d), with narrow bands separated by large gaps (red circle).

PERTURBATION THEORY

We start our analysis of the effective theory Eq. (4) by a perturbative calculation, valid for weak coupling $\gamma^2/|\omega - V \pm mv^2| \ll v\delta K$. For a lattice mismatch of $\delta \sim 1.8\%$ one has $v\delta K \gtrsim 0.22\,\text{eV}$, where the lower bound corresponds to $\theta = 0$. Since $\gamma \approx 0.3$ eV and in the absence of an external bias $|V \pm m| \gtrsim 1.5$ eV, the system is well in this perturbative regime at low energies ($|\omega| \ll |V \pm m|$ eV).

When $\eta = 1$ the model has inversion symmetry P in addition to time reversal invariance and topological arguments [14] require the presence of at least two Dirac points (or arcs) [22] in the Moiré Brillouin zone. This is the situation in twisted graphene bilayers.

When the sublattice symmetry of the substrate is broken ($\eta \neq 1$) such as through h-BN, a gap is not precluded by symmetry anymore. In the case $\zeta = 1$ it turns out that the spatial average $\langle m^{\text{eff}}\rangle = \int \mathrm{d}\mathbf{r}\, m^{\text{eff}}(\mathbf{r})$ vanishes and correspondingly no gap is found to leading order in the effective potentials. Unlike previously assumed [8, 9], this restoration of a symmetry on (spatial) average, however, does not suppress the gap in the spectrum entirely. A gap does appear at third order in $\delta H^{\text{eff}}_{\text{g}}$ [23]:

$$\Delta = \left| \eta(1-\eta)(2\cos 2\Phi - 1)\frac{\gamma^6}{81v^2\delta K^2(V - mv^2)^3} \right|. \quad (7)$$

In the more general situation, when $\zeta \neq 1$, the spatial average of the mass term $\langle m^{\text{eff}}\rangle$ is non-zero, and the band gap appears already at leading order in perturbation,

$$\Delta = \left| (1-\eta)(1-\zeta^2)\frac{\gamma^2}{3(V - mv^2)} \right|. \quad (8)$$

A recent DFT calculation [8] predicted $\Delta \approx 4\,\text{meV}$ in the absence of an external perpendicular field, when $\eta \approx -0.5$. Assuming $\gamma = 0.3\,\text{eV}$, we estimate $|1 - \zeta^2| \approx 0.14$ from Eq. (8). The relative magnitude of the local gaps in various Moiré regions found in the DFT calculation [8] indicate $\zeta > 1$, so we conclude that $\zeta \approx 1.07$. A direct fit to the local gaps of Ref. [8] in the AA-, AB-, and BA-stacked regions, respectively, yields $\zeta = 1.19$, $\eta = -0.72$, and $\gamma = 0.25\,\text{eV}$. One possible reason for the discrepancy is higher Fourier harmonics of δH^{eff} that we neglect.

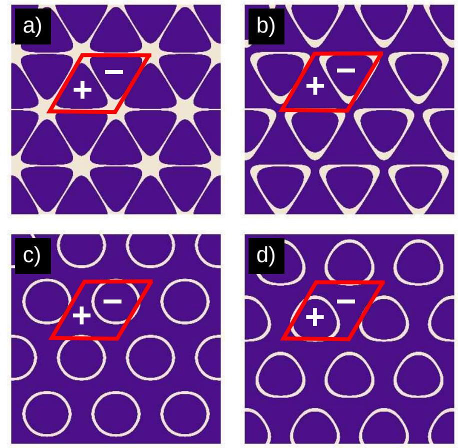

FIG. 3: Spatial dependence of the mass term resulting from the local lattice misalignment in a bilayer as shown in Fig. 1. The red line indicates the Moiré unit cell, and the $\pm$ signs specify the sign of the mass. a) $\eta = 1$: metallic state, with percolating zeros of m^{eff}; b) $\eta = 0.9$; c) $\eta = 0.5$; d) $\eta = -0.5$: the network of zeros breaks up into rings. In the strong coupling regime, those rings contain fully localized states (the states are localized by the periodic effective mass term in our low-energy theory, which opens a local gap in the blue regions of the above figure).

Eq. (8) predicts that the spectral gap of graphene on h-BN can be substantially increased by application of a perpendicular electric field that decreases the B/N on-site energies $V \pm mv^2$. As the gap increases, perturbation theory eventually breaks down, and the gap has a crossover to a nonperturbative regime.

NONPERTURBATIVE REGIME

In the nonperturbative limit $\gamma^2/|\omega - V \pm mv^2| \gg v\delta K$ the spectrum is gapped locally in regions where $m^{\text{eff}}(\mathbf{r}) \neq 0$. The low-energy physics of the system is then dominated by one-dimensional modes along the zeros of m^{eff} [17, 18]. In the absence of intervalley scattering and in the limit of a large Moiré size $L \to \infty$ these modes are guaranteed to be gapless by topological arguments [19]: the lines with $m^{\text{eff}} = 0$ separate regions with effective masses of opposite signs, as indicated by the "+" and "-" signs in Fig. 3. The massive, single-valley Dirac Hamiltonian $H = \mathbf{g}(\mathbf{k}) \cdot \boldsymbol{\sigma}$, where $\mathbf{g} = v(k_x, k_y, m^{\text{eff}}v)$ and $\boldsymbol{\sigma} = (\sigma_x, \sigma_y, \sigma_z)$, has a topological charge $N_3 = \int \mathrm{d}k_x \mathrm{d}k_y\, \hat{\mathbf{g}} \cdot \left(\partial_{k_x}\hat{\mathbf{g}} \times \partial_{k_y}\hat{\mathbf{g}}\right)/4\pi = m^{\text{eff}}/(2|m^{\text{eff}}|)$ associated with it (here, $\hat{\mathbf{g}} = \mathbf{g}/|\mathbf{g}|$). The difference of the charges N_3^+ and N_3^- to both sides of a line $m^{\text{eff}} = 0$ enforces $|N_3^+ - N_3^-| = 1$ zero modes per valley [19]. For rota-

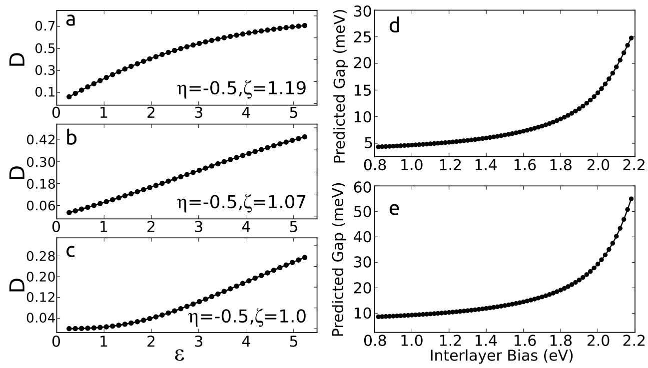

FIG. 4: Left panels: scaling function $D(\varepsilon, \eta, \zeta)$ for realistic parameter values at $\theta = 0$. The predicted crossover from linear scaling $D(\varepsilon, \eta \neq 1, \zeta \neq 1) \propto \varepsilon$ at $\zeta \neq 1$ (a,b), Eq. (8), to cubic $D(\varepsilon, \eta \neq 1, \zeta = 1) \propto \varepsilon^3$ at $\zeta = 1$ (c), Eq. (7) is confirmed. Right: Predicted gap as a function of the interlayer bias V (tunable by a perpendicular electric field) for parameter values from two fits to DFT: $\gamma = 0.3\,\mathrm{eV}$, $\eta = -0.5$, $\zeta = 1.07$ (d) and $\gamma = 0.25\,\mathrm{eV}$, $\eta = -0.72$, $\zeta = 1.19$ (e) (see text).

tional alignment $\Phi = 0$, when $\mathbf{A}^{\mathrm{eff}}$ is a pure gauge and for strong screening of the scalar potential V^{eff}, the qualitative low-energy physics thus is determined entirely by the topology of the zeros of m^{eff}.

When $\eta = 1$, such as in twisted graphene bilayers, the zeros of $m^{\mathrm{eff}}(\mathbf{r})$ form a triangular network that percolates through the entire system, as seen in Fig. 3a. The expected pairs of zero modes along these lines provide an intuitive explanation for the metallic state required by the topological arguments quoted earlier [14].

For graphene on h-BN with $\eta \neq 1$ on the other hand, this triangular network of zero energy modes breaks up into *isolated* rings (cf. Fig. 3 b-d). The low-energy modes confined to the rings of $m^{\mathrm{eff}}(\mathbf{r}) = 0$ form discrete states with an energy separation set by the circumference $C \simeq L$ of those rings. The states hosted by neighboring rings have an overlap that is exponentially small in $L\gamma^2/(V - mv^2)v$ and form correspondingly narrow (valley) pairs of bands with gaps $\Delta \approx 2\pi v/C$ in between. Evidently, in this strong coupling regime, a gap of that order of magnitude will appear regardless of whether $\langle m^{\mathrm{eff}} \rangle$ vanishes or not. This gives a physical reason why an average sublattice symmetry cannot prevent the opening of a gap in the spectrum.

For graphene on h-BN the above nonperturbative considerations do not strictly apply: there is no V such that the limit $\gamma^2/(\omega - V \pm mv^2) \gg v\delta K$ is reached for all energies ω inside the predicted gap of order $2\pi v/C \approx v\delta K \geq 220\,\mathrm{meV}$. We thus next perform numerical calculations that use a tight-binding model. Computations for the true size of the unit cell at $\theta = 0$ are challenging. We therefore exploit the scale invariance of our theory, expressing

$$\Delta = D[\gamma^2/(V - mv^2)v\delta K, \eta, \zeta] \times v\delta K \qquad (9)$$

in terms of a function $D(\varepsilon, \eta, \zeta)$ that may be evaluated for smaller unit cells [24]. The scaling parameter $\varepsilon = \gamma^2/(V - mv^2)v\delta K$ separates the weak ($\varepsilon \ll 1$) from the strong ($\varepsilon \gg 1$) coupling regime.

In Fig. 3a-c, we plot the scaling function D found from tight-binding calculations on a unit cell containing 512 atoms for typical parameters. When $\zeta = 1$, the scaling of the gap is cubic in ε for weak coupling, crossing over to linear ($\Delta \propto \varepsilon$) behavior for $\zeta \neq 1$, in agreement with the perturbative analysis of Eqs. (7) and (8). Fig. 3d-e shows the gap as a function of V for parameters taken from the two above fits to DFT data [25]. Despite the uncertainty of the parameters entering our model these calculations clearly suggest that it is possible to induce gaps in graphene on h-BN on the order of room temperature.

CONCLUSIONS

We have derived a low-energy theory for graphene on hexagonal substrates. Our theory demonstrates that a h-BN substrate opens a gap in the spectrum of graphene through a breaking of inversion symmetry even when the sublattice symmetry of graphene is restored on (spatial) average. We moreover have shown that perpendicular electric fields may be used to enhance the predicted gaps up to the scale of room temperature.

We thank A. H. Castro Neto, P. M. Goldbart, P. Jarillo-Herrero and E. J. Mele for discussions and gratefully acknowledge financial support from the NSF (DMR-1055799 and DMR-0820382). Contribution of an agency of the U.S. government, not subject to copyright.

[1] K. Novoselov, A. Geim, S. Morozov, D. Jiang, M. Katsnelson, I. Grigorieva, S. Dubonos, and A. Firsov, Nature **438**, 197 (2005).
[2] Y. Zhang, Y.-W. Tan, H. L. Stormer, and P. Kim, Nature **438**, 201 (2005).
[3] A. H. Castro Neto, F. Guinea, N. M. R. Peres, K. S. Novoselov, and A. K. Geim, Rev. Mod. Phys. **81**, 109 (2009).
[4] G. Giovannetti, P. A. Khomyakov, G. Brocks, P. J. Kelly, and J. van den Brink, Phys. Rev. B **76**, 073103 (2007).
[5] J. Sławińska, I. Zasada, and Z. Klusek, Phys. Rev. B **81**, 155433 (2010).
[6] J. Xue, J. Sanchez-Yamagishi, D. Bulmash, P. Jacquod, A. Deshpande, K. Watanabe, T. Taniguchi, P. Jarillo-Herrero, and B. LeRoy, Nature Materials **10**, 282 (2011).
[7] R. Decker, Y. Wang, V. W. Brar, W. Regan, H.-Z. Tsai, Q. Wu, W. Gannett, A. Zettl, , and M. F. Crommie, Nano Letters **11**, 2291 (2011).

[8] B. Sachs, T. O. Wehling, M. I. Katsnelson, and A. I. Lichtenstein, Phys. Rev. B **84**, 195414 (2011).
[9] C. Ortix, L. Yang, and J. van den Brink, arXiv:1111.0399 (2011).
[10] M. Yankowitz, J. Xue, D. Cormode, J. D. Sanchez-Yamagishi, K. Watanabe, T. Taniguchi, P. Jarillo-Herrero, P. Jacquod, and B. J. LeRoy, Nature physics **8**, 382 (2012).
[11] J. M. B. Lopes dos Santos, N. M. R. Peres, and A. H. Castro Neto, Phys. Rev. Lett. **99**, 256802 (2007).
[12] M. Kindermann and P. N. First, Phys. Rev. B **83**, 045425 (2011).
[13] E. J. Mele, Phys. Rev. B **84**, 235439 (2011).
[14] L. Fu and C. L. Kane, Phys. Rev. B **76**, 045302 (2007).
[15] M. S. Dresselhaus and G. Dresselhaus, Advances in Physics **51**, 1 (2002).
[16] E. J. Mele, Phys. Rev. B **81**, 161405 (2010).
[17] I. Martin, Y. M. Blanter, and A. F. Morpurgo, Phys. Rev. Lett. **100**, 036804 (2008).
[18] G. W. Semenoff, V. Semenoff, and F. Zhou, Phys. Rev. Lett. **101**, 087204 (2008).
[19] G. E. Volovik, *The Universe in a Helium Droplet*, vol. Chapter 22 (Clarendon, Oxford, 2003).
[20] In contrast to twisted graphene bilayers, where that statement does not generally hold.
[21] Provided the effective potentials are not too large [22]
[22] The argument requires that the product of the parity eigenvalues at the three M-points and the Γ-point of the Moiré Brillouin zone is -1. This condition is satisfied throughout the perturbative regime, where the effective potentials are not able to move states at M or Γ through the Fermi level [14].
[23] In case the two layers are commensurate there will be a contribution to the gap that is quadratic in γ and that is induced by a momentum-conserving term in the effective interlayer Hamiltonian of the form first pointed out by Mele [16] and neglected in our above model.
[24] Provided that the rescaled potentials $\delta H^{\rm eff} L/l$ remain smaller than the band cut-off, where the Dirac model ceases to apply.
[25] The plot neglects the ω-dependence of the effective potentials, which is a good approximation in the range of V shown in Fig. 3.